Research on Engineering Structures & Materials
www.jresm.org
Research Group

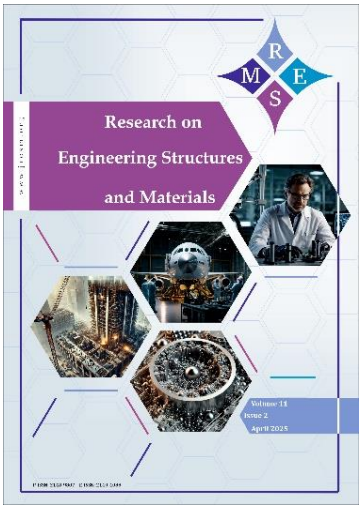


# Effect of different reinforcement methods on column-footing joint performance under seismic loading

Ibraheem H. Ridha, Bahaa H. Al-Abbas, Sadjad A. Hemzah

Online Publication Date: 30 November 2025

URL: http://www.jresm.org/archive/resm2026-1312ic1031rs.html
DOI: http://dx.doi.org/10.17515/resm2026-1312ic1031rs

Journal Abbreviation: *Res. Eng. Struct. Mater.*

**To cite this article**
Ridha I H, Al-Abbas B H, Hemzah S A. Effect of different reinforcement methods on column-footing joint performance under seismic loading. *Res. Eng. Struct. Mater.*, 2026; 12(2): 1127-1137

Research on Engineering Structures & Materials
www.jresm.org
MIM Research Group

*Research Article*

# Effect of different reinforcement methods on column-footing joint performance under seismic loading

Ibraheem H. Ridha [*,a], Bahaa H. Al-Abbas [b], Sadjad A. Hemzah [c]

*Civil Engineering Department, University of Kerbala, Karbala, Iraq*

**Article Info**

***Article History:***

Received 31 Oct 2025

Accepted 29 Nov 2025

***Keywords:***

Seismic performance;
Column-footing joint;
Reinforcement detailing;
Lateral forces;
Skeleton curve;
Axial force variation;
Modes of failure

**Abstract**

The seismic behavior of column–footing joints in reinforced concrete (RC) structures plays a critical role in ensuring structural stability under earthquake loading, especially near potential plastic hinge regions. This study aims to investigate the influence of different axial load levels and reinforcement configurations on the seismic performance of RC column–footing joints. Six specimens were cast using normal-strength concrete and subjected to reversed lateral cyclic loading. All specimens had identical dimensions, consisting of a 700 mm high column with a 120×120 mm cross-section placed on a 1000×300×200 mm footing. Two axial load levels were considered (40 and 70 kN), and the specimens were classified into three reinforcement configurations: (i) a conventional layout with stirrups and longitudinal bars, (ii) a modified design with additional longitudinal bars and connecting hoops, and (iii) a configuration with X-shaped diagonal reinforcement. Lateral loading was applied based on a processed ground motion from the 2003 Bam earthquake. Displacement was monitored using LVDTs, and performance was evaluated through skeleton curves reflecting changes in stiffness, strength, and ductility. Results showed that increasing the axial load reduced lateral resistance in reference specimens by 8.97%. The design with additional longitudinal bars and hoops maintained its strength (0.00% loss), while the X-shaped reinforcement exhibited a 5.56% strength gain. Under 40 kN axial load, the hoop-reinforced specimen improved by 13.49%, while the X-reinforced one slightly decreased by 1.46%. At 70 kN, both strengthened configurations showed substantial improvements of 24.67 and 14.27%, respectively. These findings highlight the effectiveness of longitudinal reinforcement under all axial conditions and the enhanced performance of diagonal X-bars under high axial loads, underscoring the importance of tailored reinforcement strategies for seismic resilience.



## 1. Introduction

In framed reinforced concrete (RC) structures, the column-footing joints are considered critical regions for transferring seismic and gravity loads. Under seismic actions, these joints must sustain substantial axial gravity forces while also resisting significant shear stresses arising from bending moments in beams and columns. Inadequate joint reinforcement details can result in brittle shear failures that severely compromise the integrity of the entire structural system. Observations from past earthquakes have consistently shown that insufficient detailing at these joints causes severe damage, or even structural failure. Therefore, contemporary seismic design codes mandate robust joint confinement through closely spaced transverse reinforcement, typically comprising hoops and cross-ties, to ensure ductile joint response. However, many older R.C buildings lack such joint reinforcement, prompting extensive studies on enhanced reinforcement methods [1,2]. One of the suggested methods is the placement of X-shaped diagonal reinforcement over the joint core, which reduces dependence on traditional transverse reinforcement by forming an internal truss

*Corresponding author: ibraheem.hassan@s.uokerbala.edu.iq
[a]orcid.org/0009-0006-0782-1313; [b]orcid.org/0000-0002-1362-407X; [c]orcid.org/0000-0002-1851-737X
DOI: http://dx.doi.org/10.17515/resm2026-1312ic1031rs

mechanism to effectively transfer shear stresses. This promotes ductile beam hinging over brittle joint shear failures, leading to notable increases in joint stiffness, strength, and energy dissipation capacity. It has been shown that this reinforcement approach properly shifts the failure mechanism toward beam plastic hinge zones, thus reducing joint core cracking. Interior joints with such diagonal reinforcement fastened into beams demonstrate improved lateral load resistance and post-yield stiffness compared to joints with conventional hoops.

Moreover, it was found that inclined column bars extending through the joint outperform traditional transverse stirrups in reducing joint deformation [1,3]. These results collectively support the "strong joint weak beam" design philosophy, emphasizing that diagonal reinforcement strengthens the joint panel and shifts plastic hinge formation to adjacent structural members. Despite their advantages, diagonal bars alone are not entirely adequate substitutes for transverse collars. It has been reported that joints reinforced solely with diagonal bars still suffered shear failure; however, these failures were mostly avoided by combining diagonal reinforcement with small transverse collars. Hybrid strengthening strategies have been proposed to achieve adequate confinement without overcrowding, such as combining diagonal bars with U-shaped bars at joint interfaces. These hybrid systems significantly improve load-bearing capacity and protect the joint core. Numerous experimental studies confirm that X-shaped diagonal reinforcement enhances the seismic performance of joints without altering the overall structural geometry [2,4]. Additionally, innovative retrofitting techniques using high-strength and high-ductility materials have been extensively explored. The use of high-manganese steel bars in column base joints was found to greatly enhance ductility under seismic loads. Fiber-reinforced concrete (FRC) has also been demonstrated to replace conventional stirrups to some extent, while maintaining joint strength. Engineered cementitious composites (ECCs) offer superior shear resistance and crack control compared to conventional concrete, enabling joints to tolerate higher drift demands and energy dissipation, as shown in recent experiments [5]. Other developments include hybrid reinforcement techniques and material innovations such as internal and external casing. For instance, joint cores encased with steel-covered filler composites have been shown to significantly improve ductility and shear strength. Further, combinations of capped and prestressed bars with shape memory alloys have been proposed to enhance stabilization and delay yielding [6,7].

Nevertheless, internal diagonal reinforcement remains a simple and cost-effective method to improve joint shear strength and redirect damage away from the critical core region [2,3]. Another important factor affecting joint performance is the interaction between lateral and axial loading. Seismic events dynamically change axial forces in columns and joints, thus influencing their failure modes and deformation capacities. An increase in axial load ratio from approximately 0.08 to 0.25 was found to raise joint shear strength by about 10% due to improved confinement. However, under larger axial loads (20%–60% of the column's capacity), poorly reinforced joints can exhibit brittle shear failure and reduced ductility. It has been observed that significant variations in axial loads caused by vertical seismic actions degrade hysteretic joint performance, resulting in rapid strength deterioration and brittle failure [8]. Additionally, different axial loads have been shown to alter the lateral cyclic resistance of high-strength composite columns. Under axial loads of about 70 kN, 40 kN, and 0 kN, circular sections exhibited lateral load increases of 12.96%, 19.35%, and 5.65%, respectively; whereas square sections showed increases of 6.64%, 16.63%, and 9.36%. Moreover, circular specimens provided 12.55%, 6.25%, and 10% greater resistance than square specimens under the same axial conditions. These findings further emphasize the effect of axial force levels and cross-sectional shape on the hysteretic behavior of column elements. Alternatively, very low axial forces or tension due to uplift conditions reduce confinement efficiency and may result in premature slippage of beam-bar anchorage. Finite-element analyses have shown that under low axial loads, stirrups yielded prematurely due to inadequate confinement, whereas at higher axial loads, yielding was delayed but shear stresses within the joint core intensified. Therefore, variations in axial loading substantially affect the seismic behavior of column-footing joints, influencing shear strength, failure pattern, and plastic hinge locations in either the column or the joint itself. Recent studies have examined RC joint behavior under various axial loading conditions during cyclic lateral testing to isolate axial force effects [8,10]. Findings repeatedly

demonstrate that while high axial loads tend to induce brittle failure and reduce deformation capacity, moderate axial compression enhances shear resistance [8,11].

Unlike previous studies which typically focus on beam–column joints or utilize complex retrofitting configurations and materials, the present study explores a simplified, practical approach to improving column-footing joint behavior. The objective is to evaluate the effects of different reinforcement layouts including traditional transverse reinforcement, additional longitudinal bars with hoops, and X-shaped diagonal reinforcement on seismic performance under two axial load conditions (40 kN and 70 kN). In contrast with much of the existing literature that emphasizes beam–column interaction or uses advanced materials, this study centers on applicable reinforcement details during casting, providing insights for both new construction and practical retrofitting of deficient joints.

## 2. Methodology of Research and Testing Program

This paper intends to look at how various axial loads and reinforcement detailing influence the seismic performance of column-footing joints. The approach comprises two primary specimen groups: the first under a 40 kN axial load and the second under a 70 kN axial load. It also involves material property evaluation, application of simulated seismic horizontal loads, and performance assessment. See Figure 1; the flowchart below describes the whole process in detail.

### 2.1. Testing Program

Six reinforced concrete column-footing joints were prepared, which were then split into two primary groups based on the applied axial load. While the second group comprised three specimens under an axial load of 70 kN, the first group comprised three specimens under an axial load of 40 kN. With differences in reinforcement configuration at the joint area, both groups were created with the same size and reinforcement detail. Reinforced with 12 mm diameter longitudinal bars in the column and 6 mm diameter stirrups in both the column and the footing, the first specimen in each group was a reference specimen. Consisting of extra stirrups and extra longitudinal bars with a diameter of 6 mm, the joint area of the second specimen featured more reinforcement. Diagonally main bars placed in an X-shape inside the joint area see Figure 2 strengthened the third specimen. The size of the specimens was chosen using a scale factor of five from actual short columns with full-scale dimensions of 3500 mm in height and a cross-section of 600×600 mm. The scaled specimens were therefore built with a height of 700 mm and a cross-section of 120×120 mm. Efforts were made to obtain comparable steel-to-concrete area ratios between specimens to guarantee a fair comparison between various load cases and reinforcement configurations.

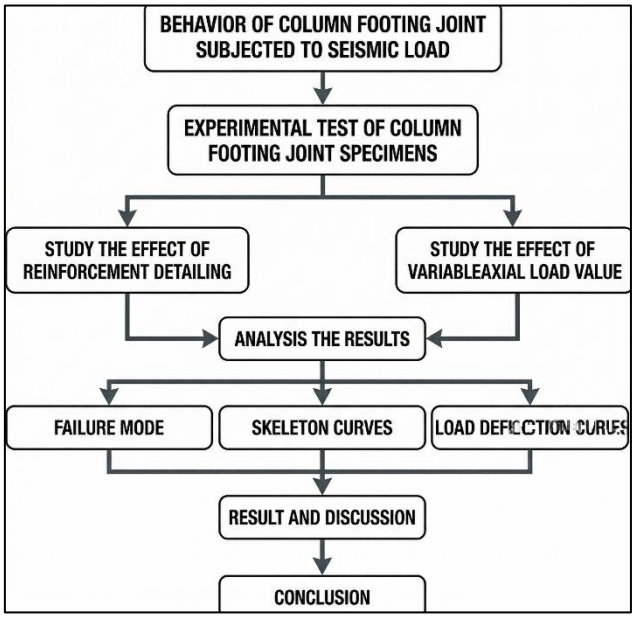


Fig. 1. Current work flowchart

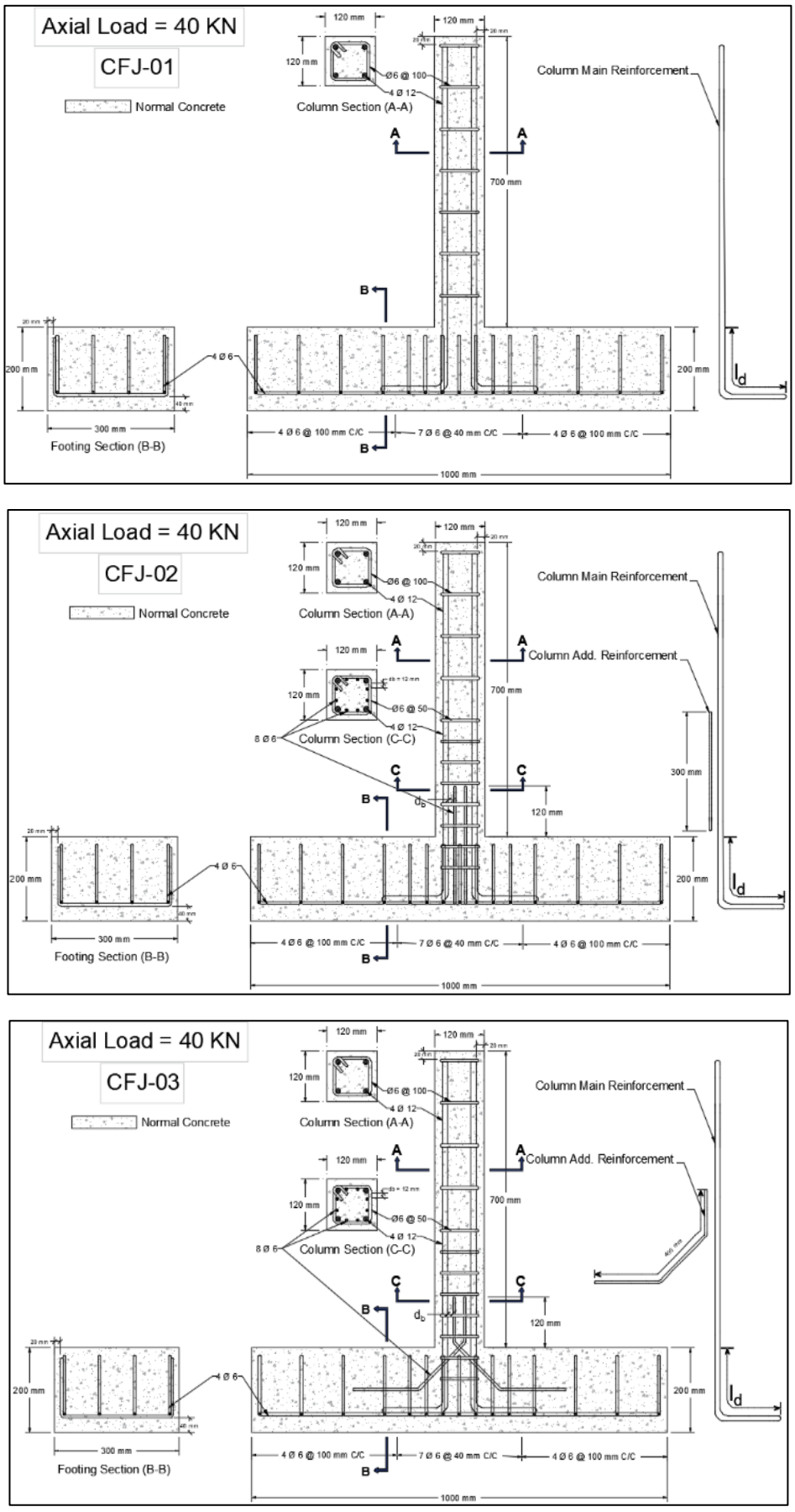


Fig. 2. Typical geometry and reinforcement details of the column–footing joint specimens (same reinforcement for all specimens; axial loads of 40 kN and 70 kN were applied) specimens

## 2.2. Materials

The concrete used in casting the column-footing joint specimens was made from a mix of cement, fine aggregate, coarse aggregate, water, and a superplasticizer. This mix was proportioned to achieve a compressive strength of about 31.4 MPa, following the guidelines of ACI 211.1 [13]. The exact quantities of the materials used in the mix are listed in Table 1.

Table 1. Concrete mix design for normal strength concrete (31.4 MPa)

| Material | Units | Value |
|---|---|---|
| Cement | kg/m$^3$ | 400 |
| Fine aggregate | kg/m$^3$ | 720 |
| Coarse aggregate | kg/m$^3$ | 1072 |
| Water | Liter | 160 |
| Superplasticizer | Liter | 6 |

The concrete casting process was performed in two separate stages. Initially, the footing parts were cast and allowed adequate time to set and gain strength. After confirming that the footings had reached sufficient hardness, the columns were then cast on top in the second stage. The cement used was Ordinary Portland Cement (OPC) Type I, with a sulfate content below 2.5% [14]. The fine aggregate belonged to Zone II according to ASTM C33 [15], while the coarse aggregate was crushed gravel with a maximum size of 14 mm [15]. These materials conformed to ASTM specifications and are commonly used in construction practices in Iraq. Following the completion of casting, all specimens were cured by immersion in water for a period of 28 days until testing. The entire experimental testing work was conducted at the laboratories of the College of Engineering, University of Karbala.

## 2.3 Properties of Concrete

A slump test using the Abrams cone technique was conducted on fresh concrete used in the column and footing joint specimens to evaluate their properties; normal strength concrete recorded a slump value of 87 mm. Three concrete cubes measuring 100×100×100 mm were cast and tested according to BS EN 12390-3 [16] to determine the 28-day compressive strength of non-homogeneous concrete (NSC). To evaluate the flexural (rupture) strength, three concrete prisms measuring 100×100×500 mm were tested according to ASTM C 78-02 [17]. Figure 3 illustrates the test procedures and specimens; Table 2 lists the results.

(a) (b9 (c8 (d)

Fig. 3. (a) Workability test (slump test), (b) concrete strength test (compressive), (d) flexural strength test (two-point loading), (c) tensile strength test (splitting method)

## 2.4 Properties of Steel Reinforcement

The columns and footings were built using deformed steel bars measuring 6 mm and 12 mm in diameter. While the 12 mm bars served as the primary longitudinal reinforcement in the columns,

the 6 mm bars were used as column stirrups and foundation reinforcement. Following the ASTM A615M-05a standard [18], a computerized testing machine in the Mechanical Engineering Laboratory at the University of Karbala was used to perform tensile tests. The 6 mm bars fulfilled the Grade 75 requirements; the 12 mm bars matched the Grade 40 based on the findings. The average mechanical properties obtained from testing three specimens of each bar type are presented in Table 3.

Table 2. Concrete compressive, splitting tensile, and flexural strength values (cylinder strength estimated as 0.8 × cube strength)

| No. | Concrete Compressive Strength, f'c (MPa) | | Splitting Tensile Strength, f'ct (MPa) | Rupture Modulus, fr (MPa) |
|---|---|---|---|---|
| | Cube | Cylinder | | |
| 1 | 43.6 | 34.9 | 2.95 | 3.89 |
| 2 | 39.5 | 31.6 | 2.82 | 3.67 |
| 3 | 34.5 | 27.6 | 2.77 | 3.75 |
| Average | 39.2 | 31.4 | 2.85 | 3.77 |

Table 3. Reinforcing steel bars' properties

| Nominal Diameter (mm) | Measured Diameter (mm) | Yield Strength (MPa) | Ultimate Strength (MPa) | Modulus of Elasticity (GPa) | Elongation (%) | ASTM A615/A615M-05a | | |
|---|---|---|---|---|---|---|---|---|
| | | | | | | Min. fy, (MPa) | Min. Elon. (%) | Grade |
| 6 | 5.5 | 658.4 | 691 | 200 | 12.1 | ≥520 | ≥7 | G75 |
| 12 | 11.83 | 419.5 | 579 | 200 | 16.3 | ≥276 | ≥12 | G40 |

## 2.5 Seismic Load Application

Seismic loading in this work was simulated using actual earthquake data from the PEER ground motion database, namely the Bam, Iran event (2003) at Mohammad Abad Madgon Station (magnitude 6.6) [19]. SeismoSignal processed the acceleration record for baseline correction and filtering to guarantee data accuracy. The Central Difference Method (CDM) was then applied to numerically calculate the lateral displacement responses under axial loads of 40 kN and 70 kN, representing one- and two-story load conditions, respectively [20]. The computed displacement waveforms were imported into LabVIEW and used during the experimental testing phase. Structural responses were monitored and recorded to evaluate performance under seismic loads. Due to the long duration of the earthquake record, only the most critical portion was selected to ensure practical application in the laboratory see Figure 4.

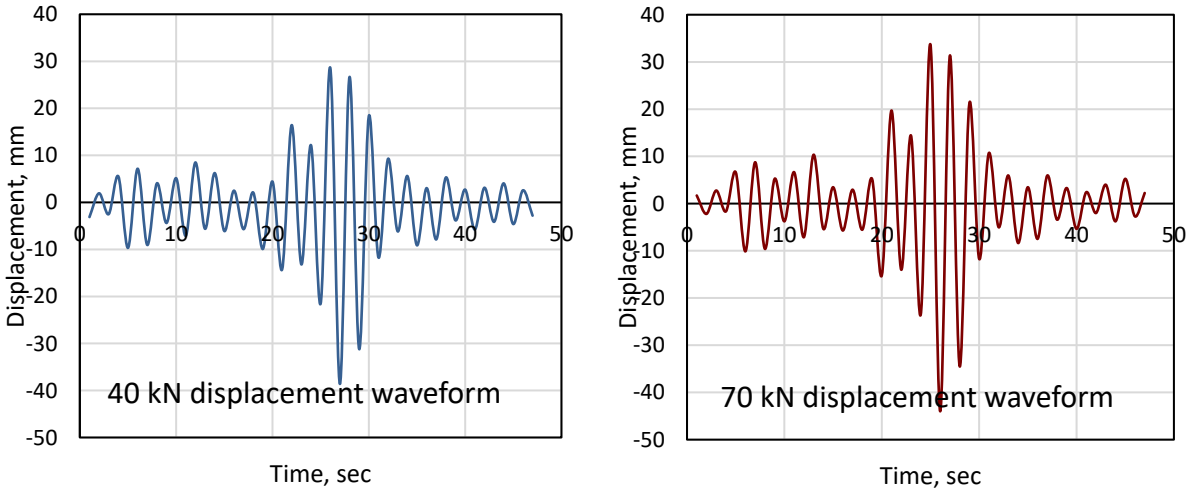


Fig. 4. Applied displacement-time patterns corresponding to 40 kN and 70 kN axial loads

## 3. Results and Discussion

The influence of reinforcement detailing on the behavior of the column-footing joint specimens under lateral loading was clearly observed during testing. To monitor the lateral displacement at the joint region, one LVDT was installed, as illustrated in Figure 5.

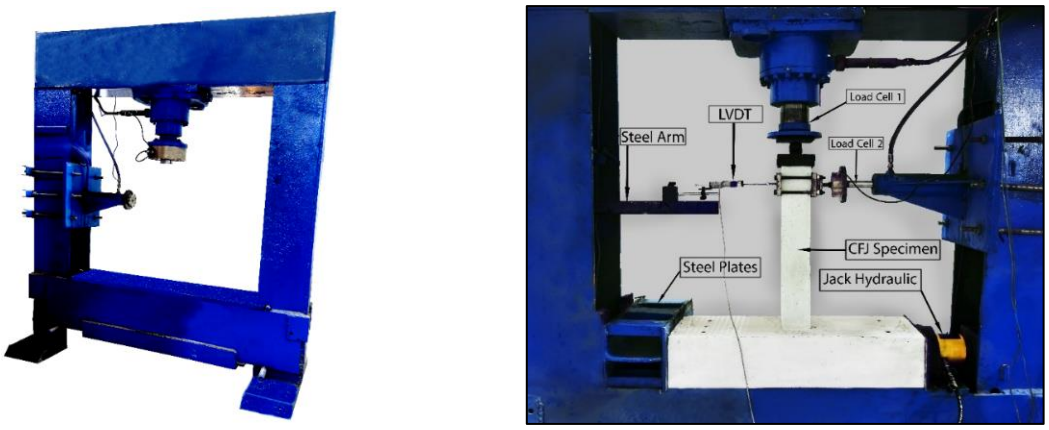


(a) (b)

Fig. 5. Test Setup: (a) general view of the testing frame and (b) specimen during testing

It was noted that as the lateral load increased, visible cracking developed in the concrete, including horizontal (latitudinal) cracks and inclined lattice-type cracks near the joint. Figure 5(a) presents the general layout of the testing frame, while Figure 5(b) shows the specific setup used for the specimens. The comparison between the different reinforcement configurations such as the addition of diagonal main bars in an X-shape, extra longitudinal bars, and additional stirrups revealed clear differences in structural response. The load–displacement curves for all tested specimens are presented in Figure 6.

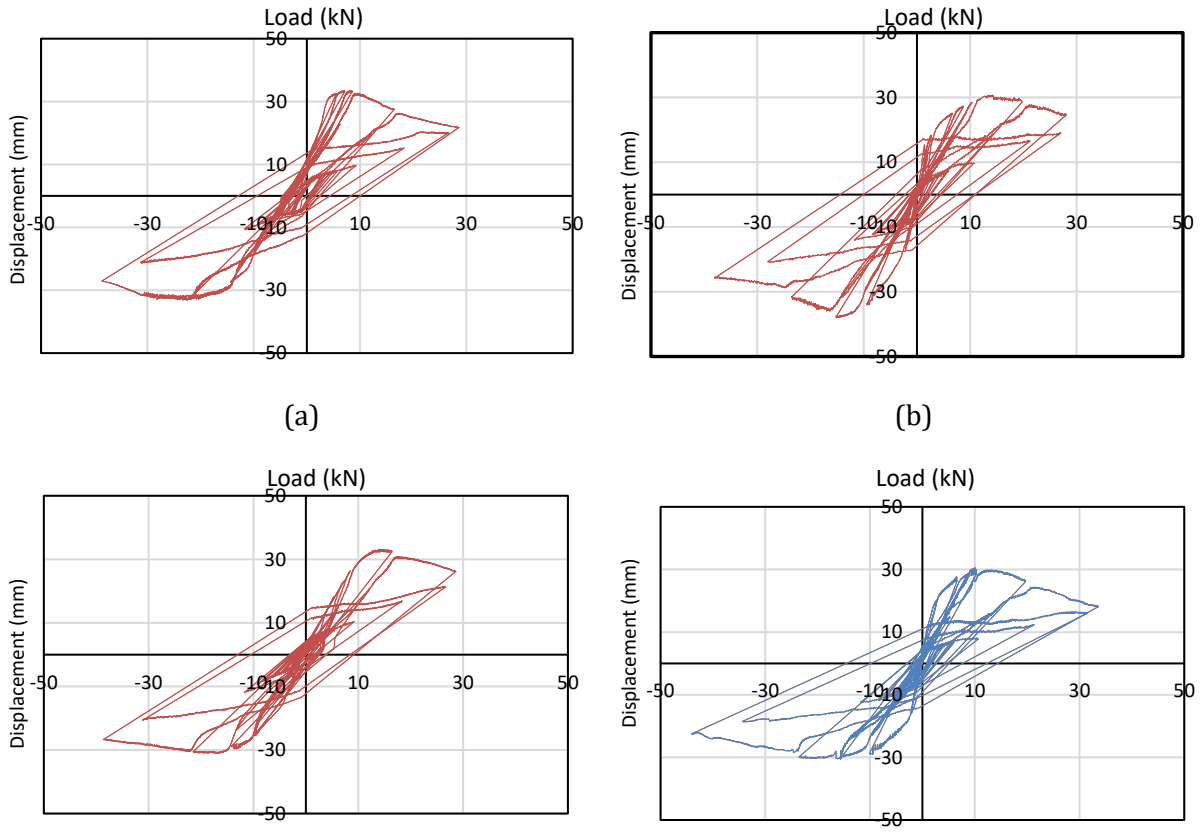


(a) (b)

(c) (d)

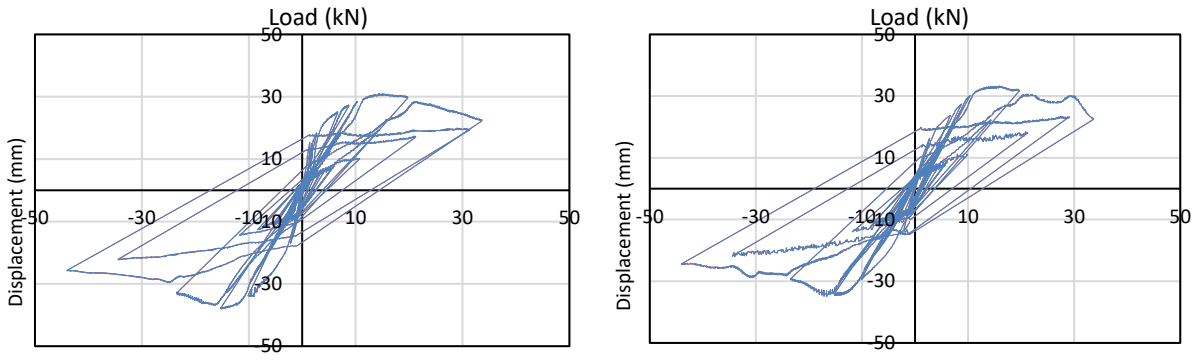


(e) (f)

Fig. 6. Lateral force–displacement response for specimens: (a) CFJ-01, (b) CFJ-02, (c) CFJ-03, (d) CFJ-07, (e) CFJ-08, (f) CFJ-09

Table 4. Results of column-footing joint specimens under lateral cyclic loading

| No. | Specimen symbol | Axial load (kN) | Maximum lateral load (kN) | Displacement at max. lateral load (mm) | Max. displacement (mm) | Lateral load at max. displacement (kN) |
|---|---|---|---|---|---|---|
| **1** | CFJ-01 | 40 | 33.57 | 7.07 | -38.57 | -27.09 |
| **2** | CFJ-02 | 40 | -38.10 | -15.15 | -38.05 | -25.81 |
| **3** | CFJ-03 | 40 | 33.08 | 14.52 | -38.67 | -26.75 |
| **4** | CFJ-07 | 70 | 30.56 | 9.99 | -44.07 | -22.49 |
| **5** | CFJ-08 | 70 | -38.10 | -15.15 | -44.01 | -25.70 |
| **6** | CFJ-09 | 70 | -34.92 | -16.64 | -44.04 | -24.39 |

### 3.1 Mode of Failure

During the test, all specimens cracked mostly in horizontal and diagonal directions in the column-footing joint area. At the joint interface, tiny cracks first developed as the lateral displacement from the earthquake wave increased, then they progressively grew and spread. Those with a 70 kN axial load experienced less but more severe fractures; these typically generated a predominant radial crack that sometimes extended to the base. At 40 kN, cracks appeared sooner and spread more widely across the joint. Reinforcement detailing was critical, with the reference specimens (CFJ-01 and CFJ-07) showing less confinement and faster crack growth, while specimens (CFJ-02 and CFJ-08) with additional longitudinal bars and collars showed more controlled and narrower cracks. Specimens with X-shaped reinforcement (CFJ-03 and CFJ-09) performed better, with less damage and delayed crack onset. By displaying the development of these cracks at different waveform phases, Figure 7 highlights how the axial load and reinforcement detailing affected the joint's failure behavior.


(a) (b)

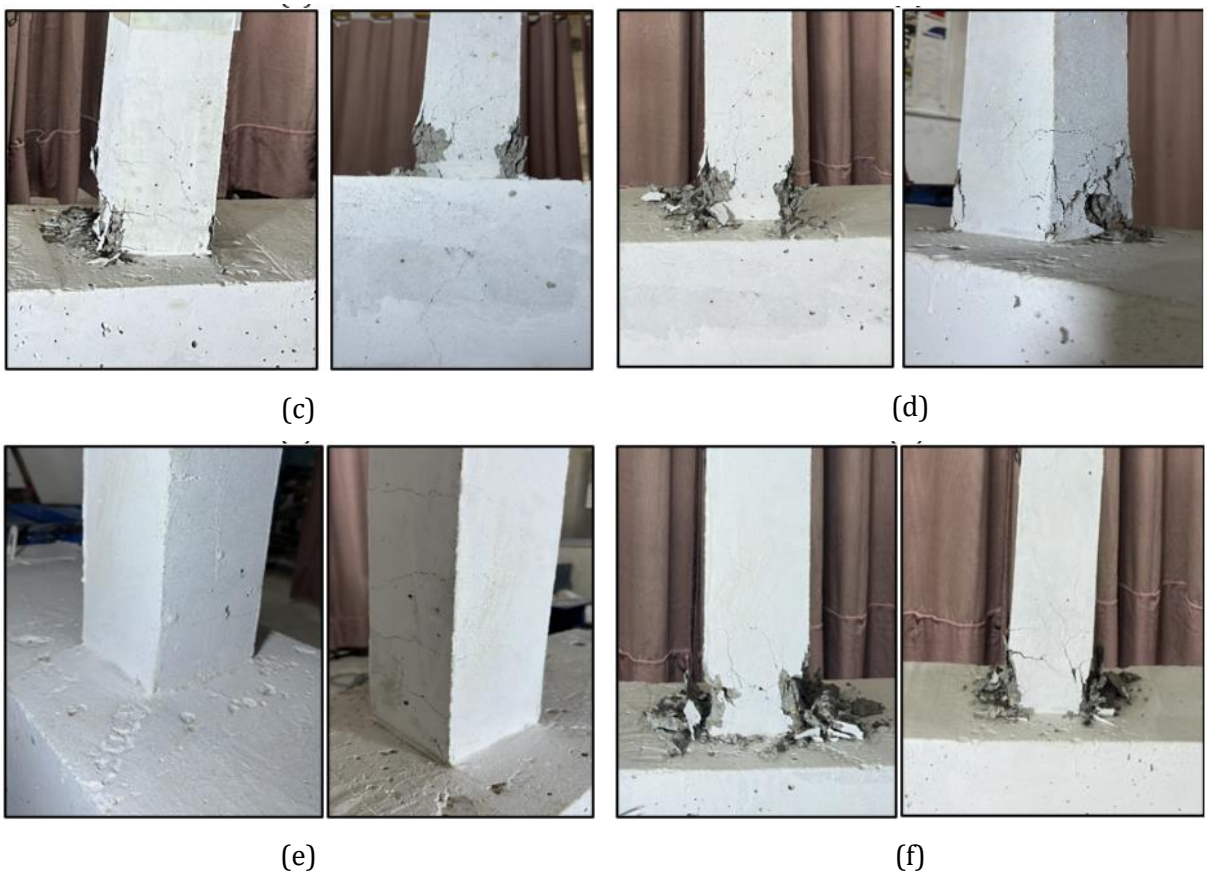


Fig. 7. Crack development in the joint area during seismic loading: (a) CFJ-01, (b) CFJ-02, (c) CFJ-03, (d) CFJ-07, (e) CFJ-08, (f) CFJ-09

### 3.2 Skelton Curves

Skeletal curves were produced by integrating the maximum lateral load and related horizontal displacement from each loading level throughout the first cycle. The skeleton curve predicts the inelastic cyclic response, deformation capacity, strength, and ductility of specimens under seismic waves. Figure 8 shows the skeleton curves for a simple comparison of the specimens.

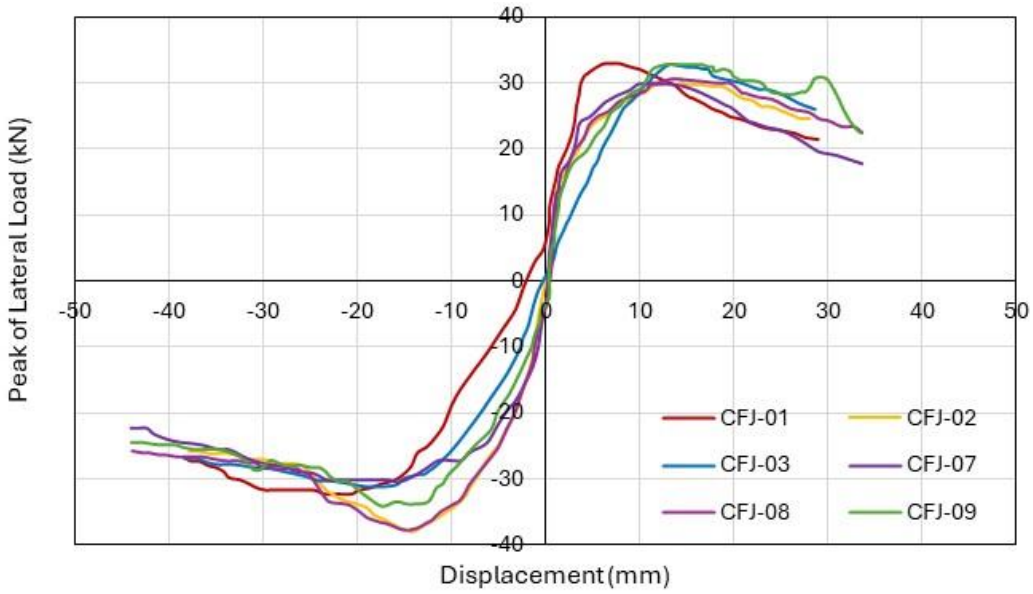


Fig. **8**. Skeleton curve for tested specimens

The behavior and results of an experimental test run under two axial load levels and reversed cyclic lateral loading on six column-footing joint specimens with variable reinforcement detailing. This study shows that:

The Impact of an Axial Load's Value. The lateral cyclic resistance was affected in different ways by raising the axial load from 40 kN to 70 kN under the same joint detailing:

- The peak lateral capacity of the reference specimen (CFJ-01 vs. CFJ-07) dropped by 8.97%.
- There was no change (0.00%) in the specimen with extra longitudinal bars and hoops (CFJ-02 vs. CFJ-08).
- There was a 5.56% increase in the specimen with diagonal X-shaped bars and hoops (CFJ-03 vs. CFJ-09).

Reinforcement Detailing's Impact.

(a)At an axial load of 40 kN (CFJ-01 baseline = 33.57 kN):

- CFJ-02 (longitudinal + hoops) gained 13.49% to 38.10 kN.
- CFJ-03 (X-shaped + hoops) dropped 1.46% to 33.08 kN.

(b) At an axial load of 70 kN (CFJ-07 baseline = 30.56 kN):

- CFJ-08 (longitudinal + hoops) gained 24.67% to 38.10 kN.
- CFJ-09 (X-shaped + hoops) gained 14.27% to 34.92 kN.

## 4. Conclusion

Axial load magnitude and reinforcement detailing on lateral cyclic resistance clearly show a correlation in the experimental data. Increasing the axial load from 40 kN to 70 kN lowered the capacity of the unstrengthen specimen by 8.97%, so increasing shear demand without confinement. The specimen having additional longitudinal bars and hoops maintained the same peak resistance at both load levels (38.10 kN) by means of efficient confinement and load redistribution. Proposing that such detail is more effective when axial compression is high, the X-shaped reinforcement enhanced performance only under higher axial load, hence increasing capacity by 5.56% compared to its 40 kN counterpart. Moreover, X-shaped bars slightly lost strength by 1.46% while longitudinal reinforcement increased it by 13.49% at 40 kN. At 70 kN, the same reinforcements increased capacity by 24.67% and 14.27% respectively. These results confirm that whereas longitudinal bars with hoops provide consistent performance under various axial conditions, X-shaped bars are more condition-sensitive.

## References

[1] Shen X, Li B, Chen YT, Tizani W. Seismic performance of reinforced concrete interior beam-column joints with novel reinforcement detail. Engineering Structures. 2021 Jan 15; 227:111408. https://doi.org/10.1016/j.engstruct.2020.111408

[2] Tiwary AK, Singh S, Chohan JS, Kumar R, Sharma S, Chattopadhyaya S, Abed F, Stepinac M. Behavior of RC beam-column joints strengthened with modified reinforcement techniques. Sustainability. 2022 Feb 8;14(3):1918. https://doi.org/10.3390/su14031918

[3] Rajagopal S, Prabavathy S. Investigation on the seismic behavior of exterior beam-column joint using T-type mechanical anchorage with hair-clip bar. Journal of King Saud University - Engineering Sciences. 2015. Online ahead of print. https://doi.org/10.1016/j.jksues.2013.09.002

[4] Tsonos AD, Kalogeropoulos G, Iakovidis P, Bezas MZ, Koumtzis M. Seismic performance of RC beam-column joints designed according to older and modern codes: An attempt to reduce conventional reinforcement using steel fiber reinforced concrete. Fibers. 2021 Apr;9(4):45. https://doi.org/10.3390/fib9070045

[5] Zhang X, Li B. Seismic performance of RC beam-column joints constructed with engineered cementitious composites. Journal of Structural Engineering. 2020 Jun;146(6):04020271. https://doi.org/10.1061/(ASCE)ST.1943-541X.0002824

[6] Dong Y, Yang X, Liu X, Qiu T, Zhou J. Seismic behavior of concrete beam-column joints reinforced with steel-jacketed grouting composite. Buildings. 2024 Oct 10;14(10):3239. https://doi.org/10.3390/buildings14103239

[7] Sharif H, Ketabi MS. An improved plastic hinge relocation technique for RC beam-column joints: Experimental and numerical investigations. Bulletin of Earthquake Engineering. 2020 Jul;18(14):4191-4225. https://doi.org/10.1007/s10518-020-00855-7
[8] Yalciner H, Kumbasaroglu A. Effect of variable axial load with different amplitude, frequency and phase on seismic behavior of RC columns: Experimental study and numerical simulation. ACI Structural Journal. 2020 Jul;117(4).
[9] Xu G, Wu B, Jia D, Xu X, Yang G. Quasi-static tests of RC columns under variable axial forces and rotations. Engineering Structures. 2018 Aug 1; 162:60-71. https://doi.org/10.1016/j.engstruct.2018.02.004
[10] Sakr MA, Seleemah AA, El-Korany T, Saad AG. Exterior beam-column joints under varying column axial load. International Journal of Advanced Structural and Geotechnical Engineering. 2019;3(2):174-186. https://doi.org/10.21608/asge.2019.270779
[11] Hu H, Chen G, Yuan H, Xu Z. Seismic strategy of non-seismically designed reinforced concrete frames under high axial load ratios. Scientific Reports. 2021 Jun 14; 11:13639.
[12] Kadhim ZF, Al-Abbas BH, Al-Khafaji AGA. Structural behavior of high-strength composite columns under lateral cyclic loads. College of Engineering, University of Kerbala. 2025. https://doi.org/10.1063/5.0236424
[13] ACI Committee 211. Standard Practice for Selecting Proportions for Normal, Heavyweight, and Mass Concrete (ACI 211.1-91). Farmington Hills (MI): American Concrete Institute; 2002.
[14] ASTM C150/C150M-22. Standard Specification for Portland Cement. West Conshohocken (PA): ASTM International; 2022.
[15] ASTM C33/C33M-18. Standard Specification for Concrete Aggregates. West Conshohocken (PA): ASTM International; 2018.
[16] British Standards Institution. BS EN 12390-3: Testing hardened concrete - Part 3: Compressive strength of test specimens. London (UK): BSI; 2019.
[17] ASTM C78-02. Standard Test Method for Flexural Strength of Concrete (Using Simple Beam with Third-Point Loading). West Conshohocken (PA): ASTM International; 2002.
[18] ASTM A615M-05a. Standard Specification for Deformed and Plain Carbon-Steel Bars for Concrete Reinforcement. West Conshohocken (PA): ASTM International; 2005.
[19] Pacific Earthquake Engineering Research Center (PEER). Ground Motion Database. University of California, Berkeley (USA).
[20] Chopra AK. Dynamics of Structures: Theory and Applications to Earthquake Engineering. 4th ed. Upper Saddle River (NJ): Prentice Hall; 2012.